A Vibration Analysis Using Numerical Results of Electromagnetic Analysis of the IPM Motor (D-model of IEEJ), Using package softwares, JMAG & CAEFEM

Takushi Fujioka*, Yoichi Tanabe
Fujitsu General Limited
fujioka.takushi@fujitsu-general.com ; tanabe.yoichi@fujitsu-general.com
TEL:+81-44-861-7767, FAX:+81-44-861-9783

Abstract :
Countermeasures for motor vibrations are an important theme in motor designs, which are involved with electrical and mechanical designs as well. We used a software package of CAEFEM and JMAG to compute the vibrations in the stator of an IPM motor (IEEJ D-model) and used electromagnetic force calculations at the condition. For this, we input the current waveforms that accounted for PWM inverter carrier harmonics into JMAG, and observed what kinds of vibrations occurred in the carrier components.

Key words Vibration analysis, Eigenvalue, FFT, Electromagnetic force, PWM control, D-model)

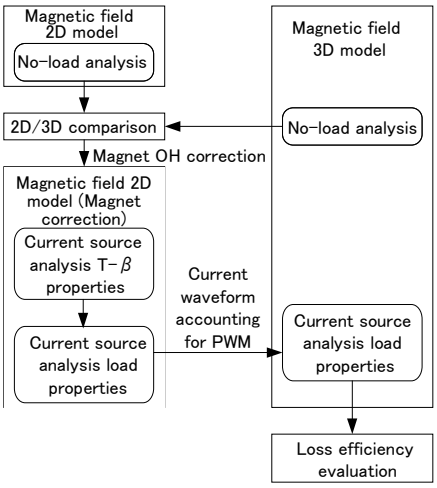

(a) Magnetic Analysis by JMAG

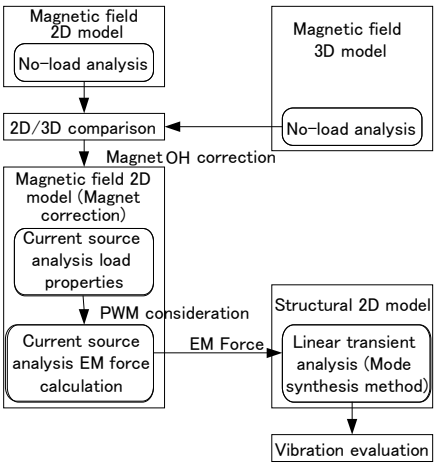

(b) Vibration Analysis by JMAG & CAEFEM

Fig.1 The Procedure of Analysis.
(From reference material 5)

1. Overview

Countermeasures for vibrations and noise in the development and design of electrical motors are an important theme for both electrical and mechanical design. In many cases, however, vibration and noise countermeasures are studied after the development and design process once a prototype has been made, so there are often times when both the degree of freedom and amount of time for studying countermeasures is greatly restricted.

In this report, I will present a method which first carries out vibration analysis using the electromagnetic force calculation results from magnetic field analysis, then calculates both the stator's eigenmode geometry and the acceleration-frequency properties, and finally evaluates the vibration. [1] The magnetic field analysis is carried out in JMAG, and the vibration analysis is done in CAEFEM. An IPM model electrical motor (IEEJ D model) is used for the benchmark motor.

In the initial stages of developing and designing an electrical motor, the advantages of vibration and noise evaluations with numerical calculations are large. At the design site we already use magnetic field vibration coupled analysis and carry out quantity production designs of IPM motors, so we hope for a wealth of case study evaluations moving forward.

2. The procedure for coupled analysis

We thought about saving time on calculations, and therefore based things on a combined approach between 2D and 3D. IPM motors do not have much flux leakage, so there are often times when you can use it with 2D problems, which means that we use 3D analysis only when it is absolutely necessary.

When we are only doing functional assessments on things like output and efficiency, we require the PWM current waveform from a 2D magnetic field analysis, so we trim down the steps and carry out 3D electric field analysis.

When carrying out vibration analysis, we implement magnetic field vibration coupling analysis. We carry out 2D magnetic field analysis in JMAG, look for the electromagnetic force (nodal force) for each point in time and create the nodal load conditions, and finally carry out 2D linear transient response structural analysis. I have shown the general process outline in fig. 1 and written it below:

〈2･1〉 Preparing for 2D electric field analysis

Compare the induced voltage between the 2D no-load analysis and 3D no-load analysis, multiply this ratio by the retention force of the 2D model's permanent magnet, and carry out corrections. Embed the effects of the overhang of the IPM rotor and the permanent magnet into the material properties with this procedure.

〈2･2〉 Deciding advanced phase angle β

Carry out 2D analysis by specifying advanced phase angle β in the sinusoidal current input, and select the β that occurs at the largest torque. With a D model, β =25(deg) is shown as the greatest value for the torque. Calculate the reluctance torque and magnetic torque by using the formula from the outcome of the no-load analysis and the load analysis. [2]

〈2･3〉 Voltage source analysis

Look for a voltage source that approximately achieves the sinusoidal curve $I_{\beta 25}$ for β =25(deg). In order to do this, first input $I_{\beta 25}$ and carry out the analysis, then

separate the basic wave components by using the Fourier transform on the voltage AC components that were output from JMAG, and after that get the total between it and the DC component $I_{\beta 25}R$ (R is the resistance between the neutral point and the terminals). Make this the voltage reference value.

With software that has no voltage output, do an inverse operation from vector potential A to get the voltage AC component. Carry out the voltage calculation for every unit of time in post-processing.

(PWM voltage reference value)=(Intra-terminal basic wave amplitude)+
+(Max. current value)×(Phase resistance)(1)

Next, carry out 2D analysis with the PWM voltage input based on the voltage reference value, and look for the PWM current waveform. This waveform contains the harmonic components from the PWM controls, so it is a similar waveform to the sinusoidal current $I_{\beta 25}$ from β =25(deg).

The time span ⊿T from the voltage source analysis decides the maximum analysis frequency f_m in the magnetic field analysis and vibration analysis. It is best to obtain ⊿T in numerical analysis by setting the f_m wave to greater than 10 divisions. Also, be careful to make sure that there are not too few steps for every carrier pulse. When implementing FFT instead of DFT, square the number of steps per period.

〈2･4〉 Current source analysis

Enter the current waveform obtained in <2･3>, and carry out magnetic field analysis. When only carrying out output and efficiency functional evaluations, skip enough steps to be able to evaluate the slot harmonics and carry out 3D analysis. When carrying out eddy current analysis on rare earth magnets, be careful not to remove so many steps that you cannot maintain the resolution performance for the Carrier Pulse. For the vibration evaluation, calculate the electromagnetic force (nodal force) for each unit of time in 2D analysis and make that the nodal load for the vibration analysis.

〈2･5〉 Vibration analysis

Process the electromagnetic force (nodal force) obtained in <2･4> and make it the nodal load. Use it to carry out real eigenmode analysis and linear transient response structural analysis. Real eigenmode analysis and transient response analysis are necessary for harmonic diagnosis that takes place during vibration analysis, so at this point we decided to use CAEFEM's structural analysis software instead of JMAG's vibration analysis module (frequency response analysis).

The (electric) frequency for transient response analysis is decided from the assumed frequency resolution (the smallest frequency that is possible to analyze).

(Periodic number)=(Mechanical speed rps) × (Number of poles)
/(Frequency resolution) (2)

Keep the wave of the frequency resolution's frequency at exactly 1 for the duration of (Period)×(Periodic number)

〈2･6〉 Fourier analysis

Run the time series data from the acceleration obtained in <2.5> through a Fourier transform, and study the vibration situation.

3. Analysis model

〈3･1〉 Motor specifications

The specifications for an IEEJ D model appear in table 1 and fig. 2. Use the simplified model.

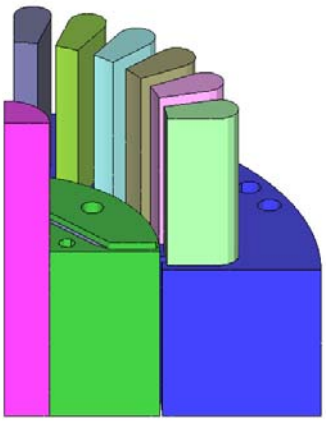

Fig.2 IEEJ D-model
(From reference material 5)

Table.1. Specification of motor
(From reference material 1)

Number of phase	3	Stack length of stator	60mm
Number of pole	4	Magnetic steel of stator	50A350
Number of slots	24	Stack length of rotor	65mm
DC Input voltage	200V	Magnetic steel of rotor	50A350
Outer diameter	112mm	Magnetization of magnet	1.25T
Length of air gap	0.5mm	Conductivity of magnet	694400S/m
Frequency of carrier	5kHz	Number of turn	35T
Number of slots	24	Resistance of phase	0.852Ω

〈3･2〉 Analysis model specifications

Fig. 3 shows a 2D magnetic field analysis model, fig. 4 shows a 3D magnetic field analysis model, and fig. 5 shows a vibration analysis model. The vibration analysis model uses the stator and outer circumference region

from the 2D magnetic field analysis model. Table 2 shows the analysis specifications.

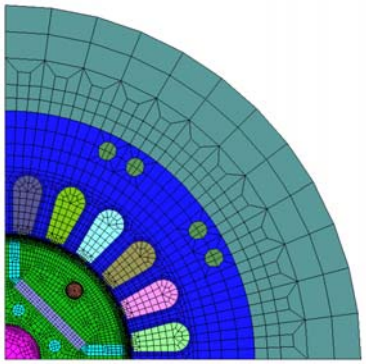

Fig. 3 Magnetic FEA model (2D).
(From reference material 5)

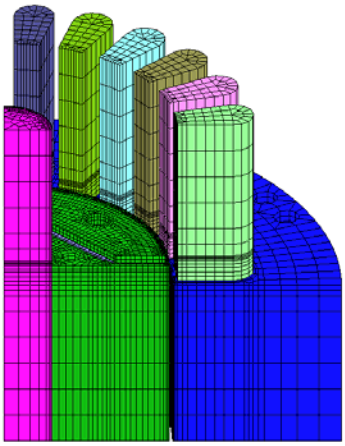

Fig. 4 Magnetic FEA model (3D).
(From reference material 5)

Table.2 Discretization data
(From reference material 5)

	Magnetic Analysis (2D)			Vib.2D
	Cur. Cntl.	Volt Cntl.	Cur. Cntl.	
No. of nodes	4784	4784	4784	5864
No. of elements	4534	4534	4534	5104
Mech.angle pitch(deg)	1.0	0.022	0.09	---
Time step pitch(μsec)	111	2.44	10	10
No. of steps per 1term	180	8192	2000	2000
No. of steps	181	24576	2000	10000
CPU time	2m12s	2h28m	47m54s	3h30m

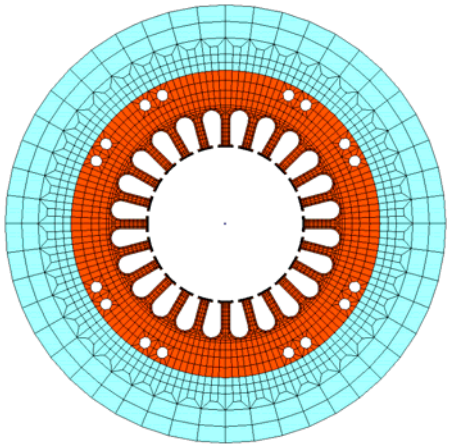

Fig. 5 Vibration analysis FEA model (2D)
(From reference material 5)

4. Analysis results

〈4･1〉 Preparations for 2D magnetic field analysis

Fig. 6 and table 3 show the results of comparing the induced voltage between 2D no-load analysis and 3D no-load analysis. There was approximately a 4.0% difference in induced voltage, and in order to correct this we carried out corrections of about 4.0% on the apparent retention force, making it M0=985245(A/m). Because of this the difference became 0.3%.

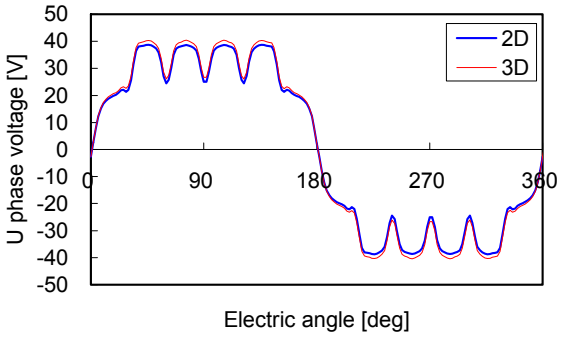

Fig.6 Electromotive Force of U phase.
(From reference material 5)

Table.3 Numerical results of Electromotive Force And Modified Magnetization
(From reference material 5)

quantities	3D	2D	2D(Modified)	Modified ratio
Br(T)	1.25	1.25	1.30	+4.0%
bHc(A/m)	947351	947351	985245	+4.0%
Max of EMF(V)	40.362	38.777	40.482	+0.3%
Effective EMF(V)	31.690	30.403	31.729	+0.1%

〈4･2〉 Deciding advanced phase angle β

Fig. 7 shows the torque obtained from carrying out 2D

analysis after setting the parameters for advanced phase angle β in the sinusoidal current input. In the D model, β = 25(deg) and the torque is the greatest value, 1.946(Nm). We made the time steps 181 for an electrical period.

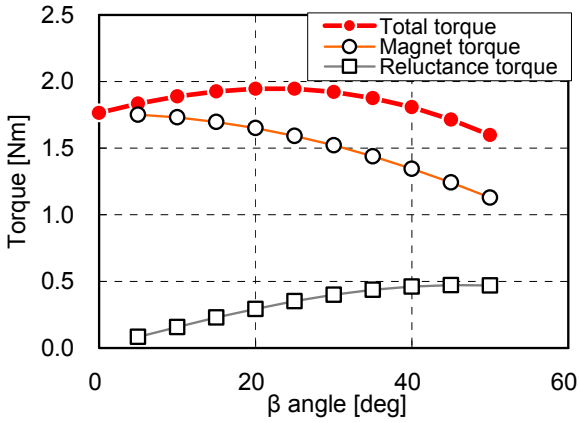

Fig.7 Torque-beta Characteristics

(From reference material 5)

〈4･3〉 Voltage source analysis

Fig. 8 shows the results from entering the sinusoidal current for β =25(deg) and doing a back calculation for the voltage current components, as well as the basic wave components separated via Fourier transform. The voltage reference value according to (1) is 96.882(Volts). We split up the time steps for the functional evaluation and vibration evaluation respectively as seen below, and calculated the current waveform. Fig. 9 shows the current waveform. The measured value agrees with the basic wave, and the trends of the harmonics fit, as well.

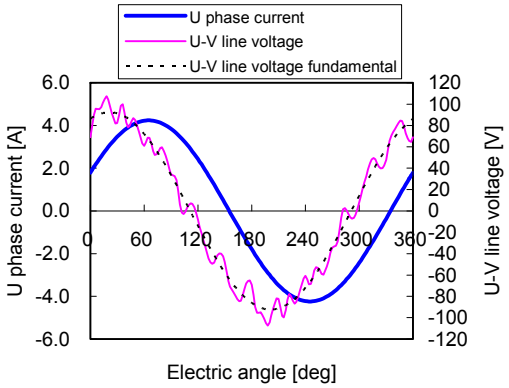

Fig.8 Fundamental mode of UV-line Volt

(From reference material 5)

(1) The number of steps for a functional evaluation

We made the electrical period 2^{13}=8192 steps. The carrier frequency was 5kHz and the mechanical speed was 1500 min^{-1} so for each electrical cycle pulse there were 100 carrier pulses, and there were 81.92 steps for each carrier pulse. In 3D analysis we used JMAG's functions and cut out steps in almost equal intervals, so there were 181 steps (Every 45.26th step).

(2) The number of steps for a vibration evaluation

Assume the audible frequencies, and set the number of steps with the frequency resolution as 10Hz and the maximum analysis frequency as 10kHz. When we set the time step interval, which divides the 10kHz wave into 10 parts, at ΔT=10μs, the mechanical speed becomes 1500 min^{-1}, so 1 electric period becomes 2000 steps. It is not squared, so we carried out Fourier analysis with DFT. Table 2 shows the analysis specifications, and fig. 10 shows the torque waveform comparison from the sine wave and PWM.

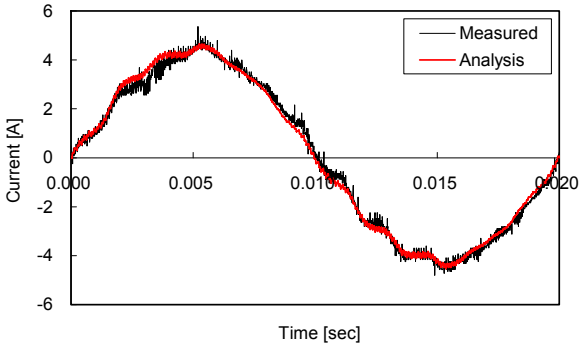

(a) Waveform

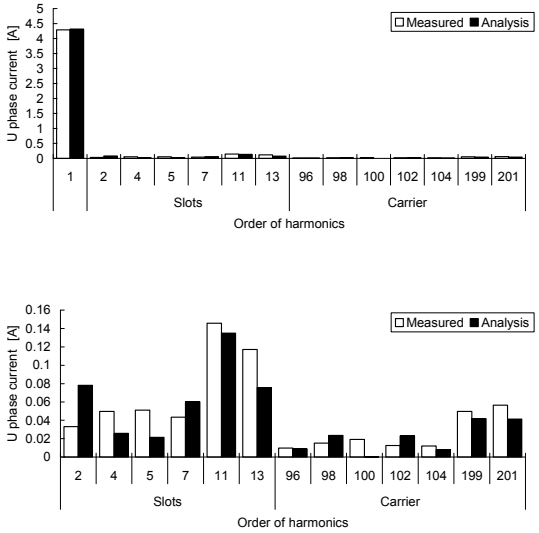

(b) Harmonics

Fig.9 Current waveform by PWM control

(From reference material 5)

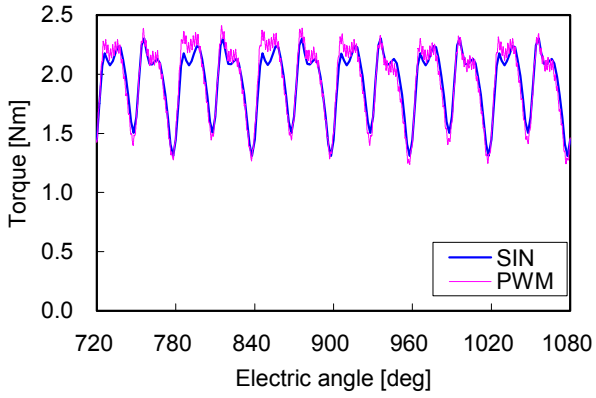

(a) Waveform

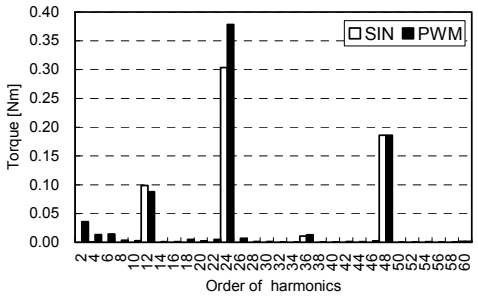

(b) Harmonics

Fig.10 Torque by SIN/PWM current

(From reference material 5)

〈4･4〉 D model functional evaluation

(1) The credibility of the evaluation

Fig. 11 shows the 3D analysis torque waveform from the thinned out steps (181 steps). The 2D and 3D waveforms match almost completely, which shows that a slot harmonic evaluation is possible.

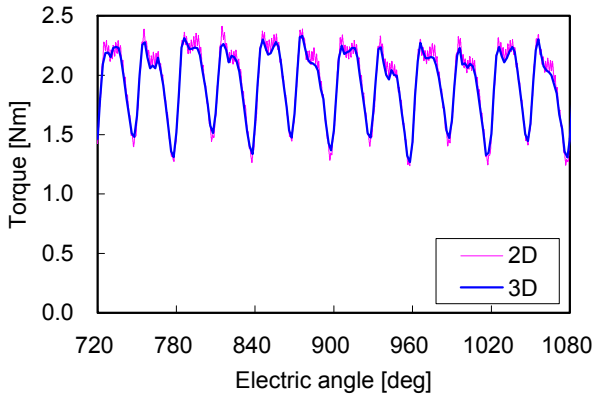

(a) Waveform

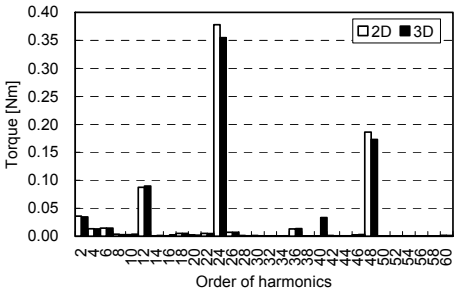

(b) Harmonics

Fig.11 Torque of 3D with curtailed time step, and Torque of 2D with original time step

(From reference material 5)

(2) Output, loss, and efficiency

The output, copper loss, iron loss, and efficiency are:

$$P_{out} = 2\pi f \cdot Torque = 2\pi \frac{1500}{60} \cdot 1.931 = 303.4(Watt) \quad (3)$$

$$W_{Cu} = (\sum_j I_j^2) \cdot R = \\ = (3.055^2 + 3.077^2 + 3.091^2) \cdot 0.852 = 24.2(Watt) \quad (4)$$

$$W_{Fe} = K_h B_{\max}^2 f + K_e B_{\max}^2 f^2 = 4.2(Watt)\,, \quad (5)$$

$$K_h = 2.012 \times 10^{-2}\,, \quad K_e = 1.512 \times 10^{-4} \quad (6)$$

$$\eta = \frac{P_{out}}{P_{out} + W_{Cue} + W_{Fe}} \times 100 = 91.4(\%)\,, \quad (7)$$

The iron loss calculation uses a method that accounts for the minor loop, and we used the recommended value from the Chiba Institute of Technology for the iron loss coefficient.

The 3D model with the thinned out steps has approximately 1.81 steps per carrier pulse, so we can calculate the slot harmonics loss, but we cannot evaluate the carrier harmonics loss. In order to resolve this, we need either to calculate the time steps without thinning them out or use the Russell coefficient on the 2D model, and make corrections like correcting with separate calculations for the magnet loss.

〈4･5〉 D model vibration evaluation

Fig. 12 shows the space distribution of the nodal force (electromagnetic force) and time changes used for the linear transient response analysis. There are 4 rotor magnetic poles, so the excitation components for the 4th special harmonic appear. Table 4 shows the material properties. The buffer material on the outer circumference was introduced because it completely anchors the outer circumference without influencing the

vibration analysis.

Table.4 Material properties

(From reference material 5)

quantities	50A350	cushioning
Young's modulus(GPa)	210	210×10-6
Mass density(kg/m3)	7650	7650×10-6
Poisson ratio	0.3	0.3

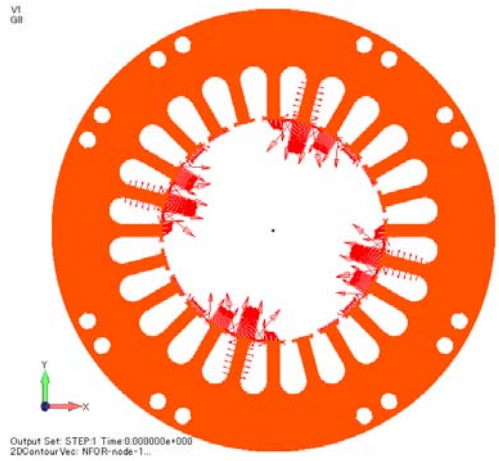

(a) 2D distribution

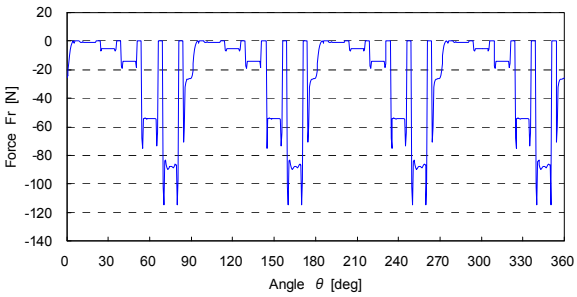

(b) Radial component Fr along the GAP

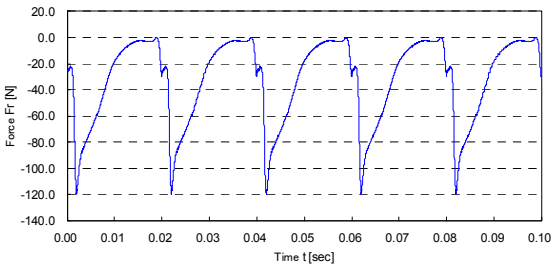

(c) Time development of Fr on a point in the Gap

Fig.12 Nodal Magnetic Force

(From reference material 5)

Fig. 13 shows the real eigenmode analysis results for the stator. The stator has eigenmodes for toroidal 2nd harmonic (3.203kHz), toroidal 3rd harmonic (8.125kHz), toroidal 4th harmonic (12.467kHz), and toroidal 0 harmonic (14.658kHz).

Fig. 14 shows Von Mises stress, acceleration response, and acceleration harmonic diagnosis according to the stator's linear transient response analysis. We made the calculations with a relaxation factor of 1%, and carried them out with the mode synthesis method.

The peak value of the toroidal 4th harmonic (12.5kHz), in which resonance appeared, was slightly less than 170dB, so when expressing it in units for auditory evaluation, the sound pressure was 54.2dB SPL, and equivalent roundness contour (fig. 15) was 40phon (On the noise judgment contour IS0226 (2003)) (4). The sound pressure notation is a reference value, so we used them for the results evaluation of the acoustic field analysis, which under normal conditions is entered as the vibration source. There is a carrier frequency 5kHz vibration at 5kHz and 10kHz, but it is excluded from the stator's eigenmode, so there is no resonance.

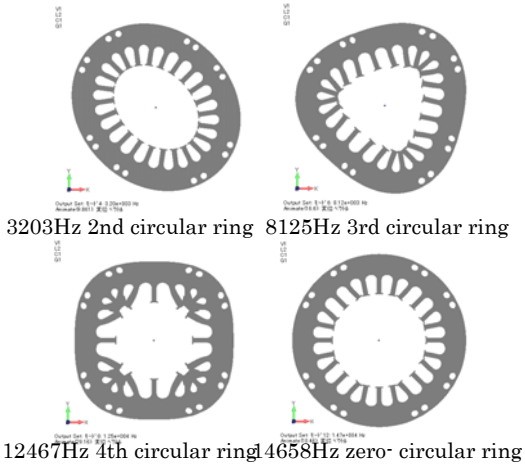

3203Hz 2nd circular ring 8125Hz 3rd circular ring

12467Hz 4th circular ring 14658Hz zero- circular ring

Fig.13 Normal mode of stators

(From reference material 5)

Fig. 16 shows acceleration distribution of the stator's outer circumference near a carrier frequency of 5kHz. The vibration mode is a toroidal 4th harmonic, and these harmonic numbers agree with the greatest common factor of the number of poles (4) and the number of slots (24).

This number is the number that occurs when the line that connects the poles of the magnet (d-axis) matches up with the line that divides the armature's teeth (4 places), and the maximum amplitude of the vibration mode appears at these places.

We understood that, generally speaking, the vibration mode harmonic number of the carrier frequency is the greatest common factor of the number of magnetic poles and the number of slots.

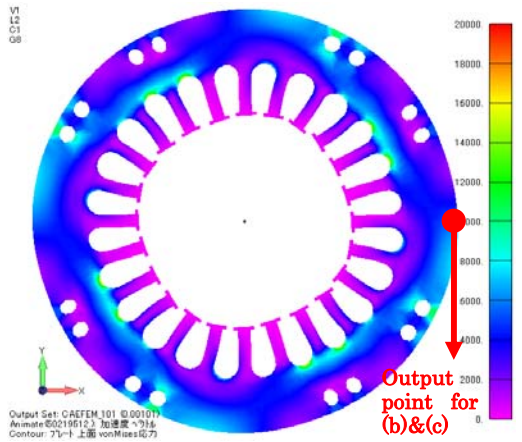

(a) von Mises' stress

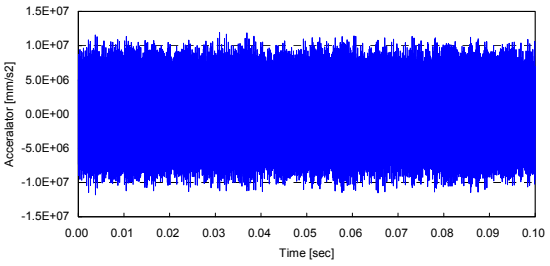

(b) Time development of acceleration

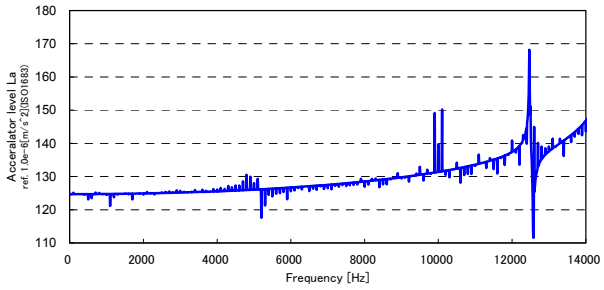

(c) DFT of computational acceleration

Fig.14 A result of Vibration Analysis

(From reference material 5)

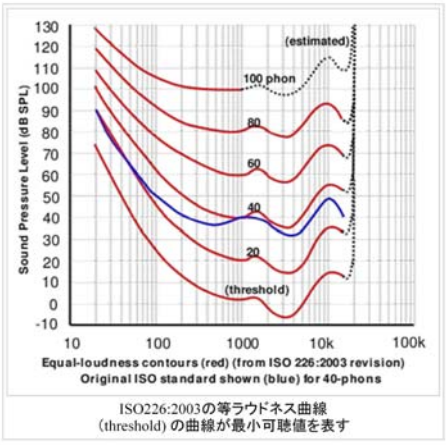

Fig.15 Equal-loudness Contours (red)

(From ISO 226-2003 revision)

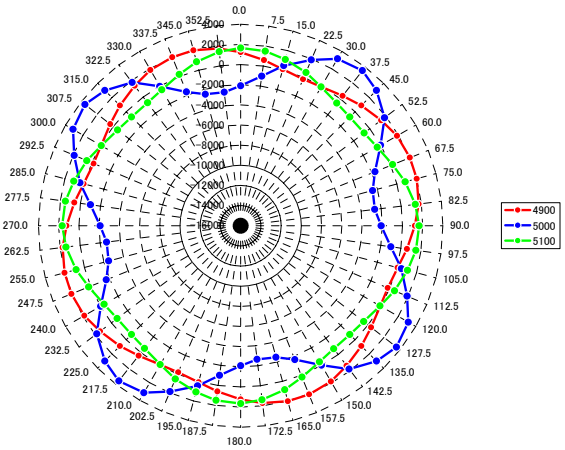

Fig.16 External mode around carrier frequency 5kHz (the outer circumference of stator)

(From reference material 5)

5. In conclusion

I have explained the procedure for magnetic field structural coupling analysis by using the D model as my main subject matter. I have shown that the D model is a motor that is highly efficient, with an efficiency of 91.4%, and that it also has superior quietness, a distribution winding characteristic.

Real eigenmode analysis and transient response analysis are necessary for harmonic diagnosis in vibration analysis, so I am hoping that from now on JMAG's vibration analysis module (frequency response analysis) will support those functions.

【Reference material】

(1) Kawase, Fujioka, Miyagi, Higuchi, Yamazaki, Akatsu, Fujita: "Industrial Application Forum's 20th Electromagnetic Field Numerical Analysis Seminar Presentation Collection," p20 (2010)

(2) Takeda, Matsui, Morimoto, Honda: "Design and Control of Embedded Magnet Synchronous Motors," Ohmsha, p16, p86(2001)

(3) K. Yamazaki, Y. Kanou, Y. Fukushima, S. Ohki, A. Nezu, T. Ikemi and R. Mizokami: "Reduction of Eddy-Current Loss in Interior Permanent-Magnet Motors With Concentrated Windings", *IEEE Trans. Ind. Appl.*, 46, 6, 2434～2441 (2010)

(4) National Astronomy Observatory of Japan: "Chronological Scientific Tables 2010," Maruzen, 428 (2009)

(5) Fujioka Takushi・Tanabe Yoichi: "One Application of Vibration Analysis Using Numerical Results of Electromagnetic Force of the IPM Motor," The Papers of Joint Technical Meeting on Static Apparatus and Rotating Machinery, IEE Japan, SA-11-026 / RM-11-026, 2011, (in Japanese)